HHS Public Access

Author manuscript

Atherosclerosis. Author manuscript; available in PMC 2018 November 01.

Published in final edited form as:

Atherosclerosis. 2017 November ; 266: 182–189. doi:10.1016/j.atherosclerosis.2017.10.009.

Lack of myeloid *Fatp1* increases atherosclerotic lesion size in *Ldlr*$^{-/-}$ mice

Liyang Zhao[a], **Alyssa J. Cozzo**[a], **Amy R. Johnson**[a], **Taylor Christensen**[a], **Alex J. Freemermana**[a], **James E. Bear**[c], **Jeremy D. Rotty**[c], **Brian J. Bennett**[d], and **Liza Makowski**[a,b,e,*]

[a]Department of Nutrition, Gillings School of Global Public Health; University of North Carolina, Chapel Hill, NC 27599, USA

[b]Department of Medicine; University of North Carolina, Chapel Hill, NC 27599, USA

[c]Lineberger Cancer Center & Department of Cell Biology and Physiology; University of North Carolina, Chapel Hill, NC 27599, USA

[d]USDA Western Human Nutrition Research Center, Davis, CA 95616, USA

[e]University of Tennessee Health Science Center, Memphis, TN 38163, USA

Abstract

Background and aims—Altered metabolism is an important regulator of macrophage (MΦ) phenotype, which contributes to inflammatory diseases such as atherosclerosis. Broadly, pro-inflammatory, classically-activated MΦs (CAM) are glycolytic while alternatively-activated MΦs (AAM) oxidize fatty acids, although overlap exists. We previously demonstrated that MΦ fatty acid transport protein 1 (FATP1, *Slc27a1*) was necessary to maintain the oxidative and anti-inflammatory AAM phenotype *in vivo* in a model of diet-induced obesity. The aim of this study was to examine how MΦ metabolic reprogramming through FATP1 ablation affects the process of atherogenesis. We hypothesized that FATP1 limits MΦ-mediated inflammation during atherogenesis. Thus, mice lacking MΦ *Fatp1* would display elevated formation of atherosclerotic lesions in a mouse model lacking the low-density lipoprotein (LDL) receptor (*Ldlr*$^{-/-}$).

Methods—We transplanted bone marrow collected from *Fatp1*$^{+/+}$ or *Fatp1*$^{-/-}$ mice into *Ldlr*$^{-/-}$ mice and fed chimeric mice a Western diet for 12 weeks. Body weight, blood glucose, and plasma

[*]***Corresponding author:*** *University of Tennessee Health Science Center*, Department of Medicine, Cancer Research Building Room 322, University of Tennessee Health Science Center, 19 South Manassas, Memphis, TN 38163. Liza.makowski@uthsc.edu*(L. Makowski).*

Conflict of interest

The authors declared they do not have anything to disclose regarding conflict of interest with respect to this manuscript.

Author contributions

L.Z, L.M designed the experiments and wrote the paper. L.Z, A.C, A.R.J, and A.J.F performed the experiments. L.Z, A.C. and T.C analyzed the data. B.J.B, J.D.R, and J.E.B developed analytical tools.

lipids were measured. Aortic sinus and aorta lesions were quantified. Atherosclerotic plaque composition, oxidative stress, and inflammation were analyzed histologically.

Results—Compared to *Fatp1*$^{+/+}$*Ldlr*$^{-/-}$ mice, *Fatp1*$^{-/-}$*Ldlr*$^{-/-}$ mice exhibited significantly larger lesion area and elevated oxidative stress and inflammation in the atherosclerotic plaque. Macrophage and smooth muscle cell content did not differ by *Fatp1* genotype. There were no significant systemic alterations in LDL, high-density lipoprotein (HDL), total cholesterol, or triacylglyceride, suggesting that the effect was local to the cells of the vessel microenvironment in a *Fatp1*-dependent manner.

Conclusions—MΦ *Fatp1* limits atherogenesis and may be a viable target to metabolically reprogram MΦs.

Keywords

FATP1; fatty acid transport protein; macrophage; metabolic reprogram; LDL receptor

1. Introduction

Macrophages (MΦs) play a central role in the pathogenesis of atherosclerosis through clearance of modified LDL particles, efferocytosis, and control of the immune milieu [1–3]. MΦs are a diverse population of cells based on site of origin, location, surface markers, functional analysis, and metabolic phenotype [4, 5]. While most work has focused on the former characteristics, little work has been conducted on understanding the metabolic phenotype of MΦs, or how MΦ metabolic phenotype influences disease progression, until recent years [6, 7]. In general, *in vitro* studies have shown that pro-inflammatory classically activated MΦs (LPS and IFNγ- stimulated, CAM or M1-like) are highly glycolytic while immunoregulatory alternatively activated MΦs (IL4-stimulated, AAM or M2-like) primarily oxidize fatty acids [8, 9]. However, *in vivo* MΦ phenotype is highly dynamic, with mixed inflammatory and metabolic phenotypes [7, 10–13].

Previous reports from our lab and others have provided evidence that when substrate metabolism is modulated, a macrophage's response to specific stimuli is dramatically altered. Fatty acid transport protein 1 (FATP1, *Slc27a1*) is an acyl-CoA synthetase wherein expression within hematopoietic populations is limited to MΦs and plasmacytoid dendritic cells [14], but not other cells that may contribute to inflammation in atherosclerosis, including monocytes, microglia, B cells, T cells, neutrophils and eosinophils [9]. We have recently reported through loss and gain of function models that FATP1 is necessary to maintain the immunoregulatory AAM phenotype *in vivo* and *ex vivo*. *Fatp1* is downregulated with pro-inflammatory stimulation of bone marrow derived MΦs [9]. Chimeric mice lacking *Fatp1* through bone marrow transplantation and fed high fat diet gained more weight and had impaired glucose tolerance on high fat diet, along with greater white adipose mass, MΦ infiltration, and crown-like structures formation. Consequently, in white adipose tissue of *Fatp1*$^{-/-}$ transplanted mice, inflammation was elevated with evidence of oxidative stress. *Fatp1*$^{-/-}$ adipose tissue MΦs (ATMs) isolated from white adipose were more CAM-like compared to ATMs isolated from *Fatp1*$^{+/+}$ transplanted mice fed a high fat diet [9]. *In vitro* studies additionally demonstrated that MΦs lacking *Fatp1* displayed a

hyper-inflammatory response to CAM stimuli, with elevations in iNOS (*Nos2*), among others, and reductions in immunoregulatory AAM marker arginase 1 (*Arg1*). Furthermore, absence of *Fatp1* led to a metabolic shift from fatty acid uptake and oxidative metabolism to increased glucose transporter GLUT1 expression, glycolysis, and metabolic intermediates associated with oxidative stress and pentose phosphate pathway [9]. Conversely, an *in vitro* gain of function model was utilized by over-expressing *Fatp1* in the RAW264.7 CAM-like MΦ cell line. RAW MΦs over-expressing *Fatp1* failed to be CAM activated, displayed blunted GLUT1 expression and reduced glucose metabolism, and exhibited increased fatty acid uptake and metabolism [9]. Thus, *Fatp1* cannot only direct the metabolic flexibility of MΦs, but the inflammatory phenotype *in vitro* and in high fat diet-exposed mice, which begs the question of the role of MΦ *Fatp1* in other metabolic diseases.

Cardiovascular diseases such as atherosclerosis are the cause of approximately 1 in 3 deaths within the United States and are the leading cause of death worldwide [15]. MΦ-mediated inflammation is a critical component of atherosclerotic plaque formation with MΦ glycolysis associated with poorer outcomes [16]. Atherosclerosis is an ongoing inflammatory process, during which MΦs mediate all stages of the disease, from initiation through progression and, ultimately, thrombotic complications, as well as resolution [1]. Our previous work indicated that there is a critical link between fatty acid transport/metabolism and inflammation in atherosclerosis, demonstrating the need to further understand novel regulators of MΦ substrate metabolism [17–20]. Because MΦ lipid metabolism plays a central role in the pathogenesis of atherosclerosis, we hypothesized that MΦs, with demonstrated blunted fatty acid metabolism and elevated glycolysis due to lack of *Fatp1*, would display increased atherogenesis. Herein, we report that while lack of hematopoietic *Fatp1* led to no systemic alterations in lipids, $Fatp1^{-/-}Ldlr^{-/-}$ mice displayed greater plaque formation, with evidence of oxidative stress and inflammation compared to $Fatp1^{+/+}Ldlr^{-/-}$ mice.

2. Materials and methods

2.1 Animals and maintenance

Animal studies were performed with approval and in accordance with the guidelines of the Institutional Animal Care and Use Committee at the University of North Carolina at Chapel Hill. Mice were housed in a climate controlled animal facility and had *ad libitium* access to food and water. $Fatp1^{-/-}$ mice [21] were provided by Dr. Andreas Stahl (University of California, Berkeley). *Fatp1* total body knockout ($Fatp1^{-/-}$) and *Fatp1* wild type ($Fatp1^{+/+}$)bone marrow donor mice were generated using $Fatp1^{-/+}$ breeding pairs to generate littermate controls. $Ldlr^{-/-}$ mice (stock number. 002207, Jackson Labs) were obtained at 4 weeks of age. At 6 weeks of age, bone marrow transplant was performed, (BMT, below). Chimeric $Ldlr^{-/-}$ mice were then housed in a sterilized environment. Mice were maintained on chow diet for four weeks before challenge with Western Diet (Harlan Teklad, TD88137) for 12 weeks.

2.2 Bone marrow transplantation

Upon arrival, N=34 4-week-old male *Ldlr*$^{-/-}$ mice were randomized to two experimental groups. At 6 weeks of age, recipient *Ldlr*$^{-/-}$ mice were administered two doses of X-ray irradiation (500cGy × 2, spaced 4 h apart; X-RAD, North Branford, CT) as in previous work [9]. Simultaneously, bone marrow was harvested from 6–8 week old male *Fatp1*$^{-/-}$ and *Fatp1*$^{+/+}$ donor mice. The femur and tibia were collected and bone marrow cells were flushed by ice-cold PBS, then centrifuged at 1,200 RPM at 4°C for 5 min. Cell pellets were resuspended in HBSS buffer. Each recipient mouse received approximately 5×10^6 bone marrow cells through retro-orbital injection under anesthesia in 100 μl. Control animals were transplanted with the HBSS buffer only, and died within 10 days of lethal irradiation.

2.3 Body weight and composition

Body weight was measured prior to starting mice on diet, and weekly until sacrifice. Body composition was measured at 6, 10, 13, 16, 19 and 22 weeks of age using the EchoMRI-100 quantitative magnetic resonance whole body composition analyzer (Echo Medical Systems, Houston, TX). Fat mass is presented as percent fat mass over total body weight [22].

2.4 Lipids and glucose measurement

After 6 h of fasting, blood was collected. Total cholesterol, LDL-cholesterol, HDL-cholesterol, and triacylglyceride were measured in the UNC Animal Clinical Chemistry and Gene Expression Core Facility by Vt350 Automated Chemical Analyzer from Ortho-Clinical Diagnostics Company (Rochester, NY). Mice were fasted for 6 h before blood glucose was measured and GTT was conducted. Blood glucose was measured using a FreeStyle Freedom Lite glucometer (Abbot Diabetes Care, Inc., Alameda, CA). Intraperitoneal GTT was performed after 7 weeks on diet at 16 weeks of age. Briefly, 2.0 gm/kg body weight of glucose was injected intraperitoneally and blood glucose was measured over 120 min [9].

2.5 Histology and quantification

Hearts were either transferred from 10% formalin to 70% ethanol stored at 4°C for creation of formalin fixed paraffin embedded (FFPE) sections or transferred to 30% sterile sucrose for 72 h for cyrosectioning. Serial interrupted sections from FFPE hearts and frozen hearts were either cut at 5 μm or 10 μm thickness. FFPE sections were stained with Masson's trichrome for quantification of collagen content, necrotic core areas, and subendothelium cell numbers, MOMA2 (macrophage/monocyte monoclonal antibody) for MΦs, anti α-SMA (alpha-smooth muscle actin) for smooth muscle cells (SMC), anti 4HNE (4-hydroxynonenal) for oxidative stress, and anti-IL6 (interleukin 6) for inflammation. The antibodies used for immunostaining were: MOMA2 (BioRad, MCA519G), anti α-SMA (Sigma, A5228), anti 4HNE (Abcam, ab48506), and anti IL6 (Novusbio, NB600-1131), which were respectively diluted as: MOMA2 (1:25), anti α-SMA (1:200), anti 4HNE (1:400), anti IL6 (1:400). The secondary antibodies were reacted with peroxidase substrate (Vectorlabs, SK-4605). Finally, slides were counterstained with methyl green. A color deconvolution algorithm, developed in collaboration with the UNC Translational Pathology Laboratory, was used to separate collagen for digital quantification (Definiens software).

Quantification of collagen was calculated as optical density (OD) × percent of total positive area stained with collagen. Necrotic core areas and subendothelial cell numbers were normalized to the total quantified areas using Aperio ePathology software (Aperio, Buffalo Grove, IL) [22–24]. Quantification of MΦ, SMC, oxidative stress, and inflammation were calculated as OD × percent of total positive area stained with MOMA2, anti α-SMA, anti 4HNE, and anti IL6 similar to previous work [22]. Frozen sections were stained with Oil red O to stain neutral lipids and hematoxylin counterstain for quantification of lesion area. Quantification of atherosclerotic lesions was performed as described [25]. Serial interrupted sections were cut through the aorta at the origins of the aortic valve leaflets, and every other section (10 μm) throughout the aortic sinus (1600 μm) was stained with Oil Red O. Aortic lesion size from each section was measured by Aperio ImageScope software. Total aortic lesion size of each animal was obtained by the summation of 5 sections from the same mouse.

2.6 Cell culture

Mouse thioglycollate-elicited peritoneal MΦs were obtained as described [20]. Using carboxylate microspheres, phagocytic capacity was measured *ex vivo* [26]. Briefly, thioglycollate-elicited peritoneal MΦs were seeded on collagen coated Nunc Lab-Tek Chamber Slide (Sigma Aldrich, St. Louis, MO) overnight. Next day, carboxylated microspheres were incubated with MΦs for either 20 min or 60 min at 37°C. Goat anti-Mouse Rhodamine red-X (Life Technologies, CA) was first incubated with cells for 15 min. Cells were then permeabilized. Goat anti-Mouse Cy5 and Alexa 488-Phalloidin (Life Technologies, CA) were then incubated with cells for another 30 min. Cells were then mounted with Fluorescent mounting media. A ZEISS LSM 700 confocal microscope was used to capture the images (UNC Microscopy Core). Phagocytosis Index (PI) was calculated by numbers of microspheres adherent to or engulfed by cells, respectively, divided by total nuclei in the field and reported as beads/cell. Experiments were repeated 3 times, with 4 technical replicates per genotype per experiment, and 2 fields/well from each experiment were captured for analysis.

2.7 Statistics

Statistical differences between experimental groups were determined by unpaired Student's *t*-tests using statistical software within GraphPad Prism (GraphPad Software, Inc., La Jolla, CA). All data are shown as mean ± standard error of the mean (SEM). *p* values less than 0.05 were considered statistically significant.

3. Results

3.1 *Fatp1*$^{+/+}$ *Ldlr*$^{-/-}$ and *Fatp1*$^{-/-}$*Ldlr*$^{-/-}$ chimeric mice gained weight and adiposity at same rates

To study the effect of *Fatp1* on mediating MΦ's contribution to atherogenesis, chimeric models were created by bone marrow transplantation (study design outlined in Supplemental Fig. 1A). Six-week-old *Ldlr*$^{-/-}$ irradiated mice were transplanted with either HBSS or bone marrow collected from *Fatp1*$^{+/+}$ or *Fatp1*$^{-/-}$ mice. Control mice transplanted with just HBSS died within 10 days (data not shown). After rescue from marrow transplant, *Fatp1*$^{+/+}$ *Ldlr*$^{-/-}$

and *Fatp1*$^{-/-}$*Ldlr*$^{-/-}$ mice were placed on western diet at 9 weeks of age and were maintained on diet until sacrifice at 22 weeks of age. There were no differences in weight gain or body composition between genotypes (Supplemental Fig. 1B and C).

3.2 Lack of *Fatp1* led to increased atherogenesis in *Fatp1*$^{-/-}$*Ldlr*$^{-/-}$ mice compared to *Fatp1*$^{+/+}$*Ldlr*$^{-/-}$ mice

After 12 weeks on western diet, mice were sacrificed and aortas were isolated and stained with Oil Red O for lesion quantification (Fig. 1A). *En face* analysis indicated that *Fatp1*$^{-/-}$*Ldlr*$^{-/-}$ mice displayed significantly greater (1.77-fold) plaque area compared to *Fatp1*$^{+/+}$*Ldlr*$^{-/-}$ mice (Fig. 1 B, p=0.001). Aortic root analysis was also conducted on sections stained with Oil Red O to determine lesion size. Aortic sinus lesion area was significantly increased by 1.72-fold in *Fatp1*$^{-/-}$*Ldlr*$^{-/-}$ mice compared to *Fatp1*$^{+/+}$*Ldlr*$^{-/-}$ mice (Fig. 2A and B, p=0.015). Deletion of *Fapt1* did not change the percent necrotic area in aortic sinus. (Fig. 2 C and D). Collagen positive area in aortic sinus was digitally quantified (Fig. 2E) and total nuclei within the subendothelium plaque area were counted (Fig. 2F); there were no *Fatp1*-mediated significant differences detected in either parameter.

3.3 There were no systemic alterations in plasma lipids or glucose tolerance in *Fatp1*$^{-/-}$*Ldlr*$^{-/-}$ mice compared to *Fatp1*$^{+/+}$*Ldlr*$^{-/-}$ *mice*

Because significant *Fatp1*-dependent differences were evident in atherogenesis, we next examined plasma lipid levels, to exclude potential systemic metabolic effects resultant from hematopoietic *Fatp1* deletion. Fig. 3 demonstrates that there were no differences in total plasma cholesterol, LDL cholesterol, HDL cholesterol or triacylglyceride in *Fatp1*$^{-/-}$*Ldlr*$^{-/-}$ mice compared to *Fatp1*$^{+/+}$*Ldlr*$^{-/-}$ mice (Fig. 3A–D). No differences in fasting blood glucose concentrations were detected from 10 to 22 weeks of age (Supplemental Fig. 2A). Likewise, a GTT was conducted at 16 weeks of age after 7 weeks on diet, which indicated that there was no genotype effect on glucose tolerance (Supplemental Fig. 2B).

3.4 Deletion of *Fatp1* did not alter plaque composition but increased oxidative stress and inflammation in atherosclerotic plaque

To further investigate potential mechanisms leading to increased lesion size, we analyzed atherosclerotic plaque cell composition and evidence of damage from oxidative stress and inflammation. IHC analysis showed that lack of *Fatp1* did not change MΦ and SMC content within the plaque as assessed by MOMA2 and αSMA staining (Fig. 4A–D). Evidence of oxidative stress was measured by 4HNE staining, which showed a significant 1.63-fold increase in *Fatp1*$^{-/-}$*Ldlr*$^{-/-}$ mice compared to *Fatp1*$^{+/+}$*Ldlr*$^{-/-}$ mice (Fig. 4E–F, p=0.013). To investigate if lacking *Fatp1* lead to increased plaque inflammation, IHC staining against IL-6 was performed. A 1.5-fold increase of IL6 staining in *Fatp1*$^{-/-}$ *Ldlr*$^{-/-}$ mice was detected compared to *Fatp1*$^{+/+}$*Ldlr*$^{-/-}$ mice (Fig. 4G–H, p=0.014).

3.5 *Fatp1* does not alter phagocytic capacity

Local MΦ function in the lesion microenvironment may also have contributed to the exacerbated atherogenesis in the absence of *Fatp1*. MΦs bind and phagocytize oxidized LDL particles in the vessel intima or debris in the lesion [27]. To investigate if *Fatp1* alters MΦ's

ability to bind particles akin to oxidized LDL, 10μM beads were used to model this behavior in thioglycollate-elicited peritoneal MΦs [28, 29]. Beads were allowed to bind for either 20 min or 60 min. Adherent and engulfed beads were quantified for each time point (Supplemental Fig. 3A and B). No significant differences were observed in adherent or engulfed beads at either time point.

4. Discussion

Increasingly, MΦ substrate metabolism has been shown to dictate inflammatory tone in complex ways as atherosclerotic lesions form and change over time [27]. Increased glucose metabolism promotes pro-inflammatory cytokines and reactive oxygen species production [9]. Classically- and alternatively-activated MΦs are detected in atherosclerotic lesions [30]. The classical M1-like MΦ has been reported to be associated with plaque progression, while the immunosuppressive alternatively-activated M2-like phenotype is associated with smaller lesions and regression of plaques [13, 16, 31–36]. We previously reported that pro-inflammatory activation is achievable by enhancing glucose metabolism via glucose transporter 1 (GLUT1) overexpression using an *in vitro* model - even in the absence of external stimuli [37] - in a demonstration of the tight immunometabolic link between MΦ metabolic reprogramming and activation state. In contrast, increased fatty acid metabolism stimulates anti-inflammatory cytokine production or blunts pro-inflammatory activation [12, 13, 38]. For example, upregulating fatty acid oxidation through inhibition of miR-33 can metabolically reprogram MΦs to the immunoregulatory AAM-like phenotype, and consequently promotes resolution of atherosclerosis [13]. Our current study supports the notion that altering MΦ fatty acid metabolism can modulate inflammatory diseases such as atherosclerosis. A critical aspect of our current work is that we demonstrate that specific deletion of FATP1 in monocyte-derived cells negatively regulates atherogenesis without disruption of systemic lipid metabolism.

Metabolic reprogramming of MΦs offers a novel means of regulating inflammation in diseases ranging from diet induced obesity and insulin resistance to cancer [39, 40]. We previously reported that metabolism of fatty acids by FATP1 played a critical role in suppressing ATM-mediated inflammation and maintaining glucose tolerance [9]. FATPs are expressed in tissues where lipid metabolism is central to the organ's function, such as adipose tissue; or where lipids provide the predominant fuel, such heart and skeletal muscle [41–43]. FATP1 activates long and very long chain FAs through its acyl-coA synthetase activity [44, 45]. Previous studies employing FATP1 total body knockout *(Fatp1*$^{-/-}$*)* mice demonstrated decreased insulin resistance, abated intramuscular accumulation of fatty acyl-CoAs, and reduced rate of diet-induced obesity when fed a high fat diet compared to *Fatp1*$^{+/+}$ mice [21, 46]. Due to its complex expression pattern, the contribution of FATP1 to the development of metabolic dysfunction is likely to be tissue- and cell-type specific. Indeed, in contrast to the whole body *Fatp1*$^{-/-}$ mice, our lab reported that chimeras created by bone marrow transplantation were more susceptible to diet-induced obesity and glucose intolerance compared to wild type transplanted mice without altering hematopoietic cell numbers [9]. We also demonstrated that there was increased MΦ infiltration, inflammatory cytokine production, and oxidative stress in the adipose tissue of mice transplanted with *Fatp1*$^{-/-}$ marrow compared to *Fatp1*$^{+/+}$ transplanted mice. Our published findings further

support the varied cell-specific roles for FATP1 which may explain the observed discrepancy in phenotype between *Fatp1*$^{-/-}$ [21, 46] and chimeric *Fatp1*$^{B-/-}$ mice [9]. Thus *Fatp1* acts as a critical metabolic hub; allowing long chain fatty acid metabolism, which in turn decreases glucose utilization [9] and associated inflammatory sequelae including oxidative stress.

MΦs play a central role in the pathogenesis of atherosclerosis, hence we further questioned whether atherogenesis can be likewise modified by altering MΦ energy metabolism and thereby phenotypic state. Through transplant of *Fatp1*$^{-/-}$ bone marrow into *Ldlr*$^{-/-}$ mice, we demonstrated a significant increase of atherosclerotic lesions in the absence of *Fatp1* by *en face* analysis. Lesions in the aortic sinus were also almost two fold larger in *Fatp1*$^{-/-}$*Ldlr*$^{-/-}$ mice compared to *Fatp1*$^{+/+}$*Ldlr*$^{-/-}$ mice. These observed differences did not appear to be due to altered plaque necrosis, collagen deposition (i.e. plaque stability), or infiltration of cells into the subendothelial space including MΦs or SMCs. Furthermore, *Fatp1*$^{-/-}$*Ldlr*$^{-/-}$ and *Fatp1*$^{+/+}$*Ldlr*$^{-/-}$ mice did not display significant differences in weight gain, glucose concentrations, or glucose tolerance on Western Diet. Importantly, plasma total cholesterol, LDL cholesterol, HDL cholesterol, and triacylglycerol concentrations also did not differ by *Fatp1* genotype. Thus, increased atherogenesis was not caused by impaired systemic lipid homeostasis but instead by increased local FATP1-dependent MΦ phenotypic changes. We next turned to an *in vitro* model to examine FATP1's contribution to macrophage's binding and phagocytic capacity since this function is essential to lesion formation, stability, and regression [27]. There were no detectable phagocytic differences driven by FATP1. In early lesions, MΦs become foam cells through engulfment of lipids, clearing neighboring dead cells (termed efferocytosis), and secretion of a spectrum of pro-inflammatory cytokines, ROS, and reactive nitrogen species (RNS). In advanced lesions, MΦs promote cell death, extracellular matrix degradation, and pro-coagulation [20, 47]. Our findings suggest that FATP1 does not regulate phagocytosis but regulates later macrophage functions including cytokine and ROS production, although the mechanisms remain unclear.

Finally, we focused on the established role of FATP1 in maintaining the immunoregulatory AAM phenotype [9]. FATP1 directs substrate metabolism in MΦs - when MΦs lack *Fatp1*, cells switch from oxidation of fatty acids to increased glucose utilization through elevated glycolysis, an indicator of a CAM/M1-like pro-inflammatory activation phenotype [9]; when MΦs overexpressed *Fatp1*, cells displayed reduced glycolytic capacity and glucose oxidation, a marker of AAM/M2-like immunomodulatory phenotype [9]. Our lab previously reported that RAW264.7 MΦs overexpressing *Fatp1* secreted significantly less IL6 compared to control MΦs, further demonstrating the importance of FATP1 in the regulation of MΦ phenotype [9]. In the current loss of function study, we detected significantly increased IL6 staining in aortic root lesions of *Fatp1*$^{-/-}$ *Ldlr*$^{-/-}$ mice, suggesting that FATP1 typically acts to limit inflammation and here lack of MΦ *Fatp1* promoted lesion cytokine production. Our lab previously reported that *Fatp1*$^{-/-}$ MΦs expressed increased iNOS *(Nos2)* and TNFα *(Tnfa)*, as well as significantly reduced arginase1 (*Arg1*) [9]. Nitric oxide and TNFα accelerate atherogenesis [48], while the expression of arginase I (a marker of AAM/M2-like MΦs) decelerates atherogenesis [49]. Expression of pro-inflammatory cytokines is often co-incident with oxidative damage. In our previously published work, increased oxidative damage was detected in white adipose tissue of mice transplanted with *Fatp1*$^{-/-}$ marrow and made obese compared to mice transplanted with control *Fatp1*$^{+/+}$

marrow. Importantly, herein we found that mice lacking MΦ *Fatp1* displayed significantly increased 4HNE staining in the aortic root plaque, indicating that deletion of macrophage FATP1 exacerbated lesion oxidative stress. In conclusion, our data showed increased atherogenesis in $Fatp1^{-/-}Ldlr^{-/-}$ mice, caused by deletion of *Fatp1*-mediated local inflammation and oxidative stress compared to $Fatp1^{+/+}Ldlr^{-/-}$ mice. However, several limitations to this study should be taken into account with regard to this work. First, our previous work studying FATP1 was in mice fed a high fat diet [9], which is different from the Western diet utilized herein and may limit comparisons across studies. Second, previous hematologic characterization of blood cells from $Fatp1^{+/+}$ and $Fatp1^{-/-}$ mice [9] may inform atherosclerotic findings, yet future analysis is imperative specifically in mice lacking *Fatp1* in the $Ldlr^{-/-}$ background to determine if the loss of FATP1 in the $Ldlr^{-/-}$ background alters the immune cell composition that may explain findings herein. Finally, we have extrapolated from previous work using typical stimuli (LPS/IFNγ or IL4) to model *in vitro* extremes of the MΦ polarization spectrum. Yet, it is possible that when macrophages are challenged with lipids such as oxidized or acetylated LDL or apoptotic foam cells which are more relevant to the atherosclerotic lesion, different phenotypes may emerge. Ideally, single cell RNA sequencing should be conducted on macrophages from lesions to best understand the *in vivo* phenotype and are planned for future studies.

Our data provides new findings linking substrate utilization, macrophage function, and disease susceptibility in mouse models, which implicate MΦ expression of *Fatp1* as a critical mediator of these processes. Our hypothesis regarding MΦ FATP1 driving macrophage phenotype and atherosclerosis is difficult to prove in human studies but there are important clues that this may in fact be the case. A common gene variant exists in *SLC27A1* and is associated with elevated post-prandial lipemia and alterations in LDL particle size distribution [50]. There are also reports of *Fatp1* genomic variants affecting the levels of FATP1 mRNA, a putative cis-eQTL, in the Metabolic Syndromes In Men (METSIM) study [9, 51]. More recent data from the GTEx portal indicates that there is complex, tissue-specific genetic regulation of FATP1 [52] and a wider distribution of expression than originally understood. These data suggest that FATP1 expression varies in humans based on genotype and some FATP1 alleles are associated with cardiovascular disease related phenotypes. Further study specifically targeting macrophage metabolic phenotypes is needed to fully understand mechanisms linking fatty acid transport proteins and macrophages in cardiovascular outcomes.

Supplementary Material

Refer to Web version on PubMed Central for supplementary material.

Acknowledgments

We thank Dr. Andreas Stahl for generously providing us with the $Fatp1^{-/-}$ mice. Histological services were provided by the Histology Research Core Facility in the Department of Cell Biology and Physiology at the University of North Carolina Chapel Hill NC.

Financial support

Alyssa Cozzo-Chancellor's Scholarship, Royster Society of Fellows; McAllister Heart Institute T32 - Pre- Doctoral Training Program in Integrative Vascular Biology. Amy Rose Johnson-NIH F32H117616. Jim Bear-NIH Grant GM083035. Jeremy Rotty-NIH Grant GM083035. Brian Bennett-5R01HL128572-02. Liza Makowski- AHA grant 13BGIA17070106 and MHI grant Scott Custer Cardiology Seed Grant Fund

References

1. Tabas I, Garcia-Cardena G, Owens GK. Recent insights into the cellular biology of atherosclerosis. J Cell Biol. 2015; 209(1):13–22. [PubMed: 25869663]
2. Schaftenaar F, et al. Atherosclerosis: the interplay between lipids and immune cells. Curr Opin Lipidol. 2016; 27(3):209–15. [PubMed: 27031276]
3. von Scheidt M, et al. Applications and Limitations of Mouse Models for Understanding Human Atherosclerosis. Cell Metab. 2016
4. Davies LC, et al. Tissue-resident macrophages. Nat Immunol. 2013; 14(10):986–95. [PubMed: 24048120]
5. Gordon S, Pluddemann A, Martinez Estrada F. Macrophage heterogeneity in tissues: phenotypic diversity and functions. Immunol Rev. 2014; 262(1):36–55. [PubMed: 25319326]
6. Rodriguez-Prados JC, et al. Substrate fate in activated macrophages: a comparison between innate, classic, and alternative activation. J Immunol. 2010; 185(1):605–14. [PubMed: 20498354]
7. Van den Bossche J, O'Neill LA, Menon D. Macrophage Immunometabolism: Where Are We (Going)? Trends Immunol. 2017; 38(6):395–406. [PubMed: 28396078]
8. Johnson AR, Milner JJ, Makowski L. The inflammation highway: metabolism accelerates inflammatory traffic in obesity. Immunologic Reviews. 2012; 249(1):218–238.
9. Johnson AR, et al. Metabolic reprogramming through fatty acid transport protein 1 (FATP1) regulates macrophage inflammatory potential and adipose inflammation. Mol Metab. 2016; 5(7): 506–26. [PubMed: 27408776]
10. Kelly B, O'Neill LA. Metabolic reprogramming in macrophages and dendritic cells in innate immunity. Cell Res. 2015; 25(7):771–84. [PubMed: 26045163]
11. O'Neill LA, Pearce EJ. Immunometabolism governs dendritic cell and macrophage function. J Exp Med. 2016; 213(1):15–23. [PubMed: 26694970]
12. Vats D, et al. Oxidative metabolism and PGC-1beta attenuate macrophage-mediated inflammation. Cell Metab. 2006; 4(1):13–24. [PubMed: 16814729]
13. Ouimet M, et al. MicroRNA-33-dependent regulation of macrophage metabolism directs immune cell polarization in atherosclerosis. J Clin Invest. 2015; 125(12):4334–48. [PubMed: 26517695]
14. https://www.immgen.org/.
15. Writing Group, M. Heart Disease and Stroke Statistics-2016 Update: A Report From the American Heart Association. Circulation. 2016; 133(4):e38–360. [PubMed: 26673558]
16. Shirai T, et al. The glycolytic enzyme PKM2 bridges metabolic and inflammatory dysfunction in coronary artery disease. J Exp Med. 2016; 213(3):337–54. [PubMed: 26926996]
17. Makowski L, et al. Lack of macrophage fatty-acid-binding protein aP2 protects mice deficient in apolipoprotein E against atherosclerosis. Nat Med. 2001; 7(6):699–705. [PubMed: 11385507]
18. Makowski L, et al. The fatty acid-binding protein, aP2, coordinates macrophage cholesterol trafficking and inflammatory activity. Macrophage expression of aP2 impacts peroxisome proliferator-activated receptor gamma and IkappaB kinase activities. J Biol Chem. 2005; 280(13): 12888–95. [PubMed: 15684432]
19. Furuhashi M, et al. Treatment of diabetes and atherosclerosis by inhibiting fatty-acid-binding protein aP2. Nature. 2007; 447(7147):959–65. [PubMed: 17554340]
20. Erbay E, et al. Reducing endoplasmic reticulum stress through a macrophage lipid chaperone alleviates atherosclerosis. Nat Med. 2009; 15(12):1383–91. [PubMed: 19966778]
21. Kim JK, et al. Inactivation of fatty acid transport protein 1 prevents fat-induced insulin resistance in skeletal muscle. J Clin Invest. 2004; 113(5):756–63. [PubMed: 14991074]
22. Sundaram S, et al. Role of HGF in obesity-associated tumorigenesis: C3(1)-TAg mice as a model for human basal-like breast cancer. Breast Cancer Res Treat. 2013; 142(3):489–503. [PubMed: 24218051]

23. Sundaram S, et al. Weight Loss Reversed Obesity-Induced HGF/c-Met Pathway and Basal-Like Breast Cancer Progression. Front Oncol. 2014; 4:175. [PubMed: 25072025]
24. Cozzo AJ, et al. cMET inhibitor crizotinib impairs angiogenesis and reduces tumor burden in the C3(1)-Tag model of basal-like breast cancer. Springerplus. 2016; 5:348. [PubMed: 27057482]
25. Daugherty A, Whitman SC. Quantification of atherosclerosis in mice. Methods Mol Biol. 2003; 209:293–309. [PubMed: 12357958]
26. DeLoid GM, et al. Heterogeneity in macrophage phagocytosis of Staphylococcus aureus strains: high-throughput scanning cytometry-based analysis. PLoS One. 2009; 4(7):e6209. [PubMed: 19593389]
27. Tabas I, Bornfeldt KE. Macrophage Phenotype and Function in Different Stages of Atherosclerosis. Circ Res. 2016; 118(4):653–67. [PubMed: 26892964]
28. Lewkowicz E, et al. The microtubule-binding protein CLIP-170 coordinates mDia1 and actin reorganization during CR3-mediated phagocytosis. J Cell Biol. 2008; 183(7):1287–98. [PubMed: 19114595]
29. Sano H, et al. Critical role of galectin-3 in phagocytosis by macrophages. J Clin Invest. 2003; 112(3):389–97. [PubMed: 12897206]
30. Stoger JL, et al. Distribution of macrophage polarization markers in human atherosclerosis. Atherosclerosis. 2012; 225(2):461–8. [PubMed: 23078881]
31. Feig JE, et al. HDL promotes rapid atherosclerosis regression in mice and alters inflammatory properties of plaque monocyte-derived cells. Proc Natl Acad Sci U S A. 2011; 108(17):7166–71. [PubMed: 21482781]
32. Feig JE, et al. Reversal of hyperlipidemia with a genetic switch favorably affects the content and inflammatory state of macrophages in atherosclerotic plaques. Circulation. 2011; 123(9):989–98. [PubMed: 21339485]
33. Cardilo-Reis L, et al. Interleukin-13 protects from atherosclerosis and modulates plaque composition by skewing the macrophage phenotype. EMBO Mol Med. 2012; 4(10):1072–86. [PubMed: 23027612]
34. Hanna RN, et al. NR4A1 (Nur77) deletion polarizes macrophages toward an inflammatory phenotype and increases atherosclerosis. Circ Res. 2012; 110(3):416–27. [PubMed: 22194622]
35. Sharma N, et al. Myeloid Kruppel-like factor 4 deficiency augments atherogenesis in ApoE−/− mice--brief report. Arterioscler Thromb Vasc Biol. 2012; 32(12):2836–8. [PubMed: 23065827]
36. Sarrazy V, et al. Disruption of Glut1 in Hematopoietic Stem Cells Prevents Myelopoiesis and Enhanced Glucose Flux in Atheromatous Plaques of ApoE(−/−) Mice. Circ Res. 2016; 118(7): 1062–77. [PubMed: 26926469]
37. Sundaram S, et al. Obesity-mediated regulation of HGF/c-Met is associated with reduced basal-like breast cancer latency in parous mice. PLoS One. 2014; 9(10):e111394. [PubMed: 25354395]
38. Freemerman AJ, et al. Metabolic Reprogramming of Macrophages: Glucose transporter 1 (GLUT1)-mediated glucose metabolism drives a pro-inflammatory phenotype. J Biol Chem. 2014; 289(11):7884–96. [PubMed: 24492615]
39. Kaneda MM, et al. PI3Kgamma is a molecular switch that controls immune suppression. Nature. 2016; 539(7629):437–442. [PubMed: 27642729]
40. Mantovani A, Locati M. Macrophage Metabolism Shapes Angiogenesis in Tumors. Cell Metab. 2016; 24(6):887–888. [PubMed: 27974181]
41. Schaffer JE, Lodish HF. Expression cloning and characterization of a novel adipocyte long chain fatty acid transport protein. Cell. 1994; 79(3):427–36. [PubMed: 7954810]
42. Hirsch D, Stahl A, Lodish HF. A family of fatty acid transporters conserved from mycobacterium to man. Proc Natl Acad Sci U S A. 1998; 95(15):8625–9. [PubMed: 9671728]
43. Binnert C, et al. Fatty acid transport protein-1 mRNA expression in skeletal muscle and in adipose tissue in humans. Am J Physiol Endocrinol Metab. 2000; 279(5):E1072–9. [PubMed: 11052962]
44. Hall AM, Smith AJ, Bernlohr DA. Characterization of the Acyl-CoA synthetase activity of purified murine fatty acid transport protein 1. J Biol Chem. 2003; 278(44):43008–13. [PubMed: 12937175]
45. Coe NR, et al. The fatty acid transport protein (FATP1) is a very long chain acyl-CoA synthetase. J Biol Chem. 1999; 274(51):36300–4. [PubMed: 10593920]

46. Wu Q, et al. FATP1 is an insulin-sensitive fatty acid transporter involved in diet-induced obesity. Mol Cell Biol. 2006; 26(9):3455–67. [PubMed: 16611988]

47. Hopkins PN. Molecular biology of atherosclerosis. Physiol Rev. 2013; 93(3):1317–542. [PubMed: 23899566]

48. Kleinbongard P, Heusch G, Schulz R. TNFalpha in atherosclerosis, myocardial ischemia/reperfusion and heart failure. Pharmacol Ther. 2010; 127(3):295–314. [PubMed: 20621692]

49. Wang XP, et al. Arginase I enhances atherosclerotic plaque stabilization by inhibiting inflammation and promoting smooth muscle cell proliferation. Eur Heart J. 2014; 35(14):911–9. [PubMed: 23999450]

50. Gertow K, et al. A common polymorphism in the fatty acid transport protein-1 gene associated with elevated post-prandial lipaemia and alterations in LDL particle size distribution. Atherosclerosis. 2003; 167(2):265–73. [PubMed: 12818409]

51. Mahendran Y, et al. Association of ketone body levels with hyperglycemia and type 2 diabetes in 9,398 Finnish men. Diabetes. 2013; 62(10):3618–26. [PubMed: 23557707]

52. Freemerman AJ, et al. Metabolic reprogramming of macrophages: glucose transporter 1 (GLUT1)-mediated glucose metabolism drives a proinflammatory phenotype. J Biol Chem. 2014; 289(11):7884–96. [PubMed: 24492615]

Highlights

- Lack of *Fatp1* led to increased atherosclerotic lesions in $Ldlr^{-/-}$ mice
- Larger lesions in $Fatp1^{-/-}$ $Ldlr^{-/-}$ mice were not due to systemic changes in lipids
- Lesions in $Fatp1^{-/-}$ $Ldlr^{-/-}$ mice had greater oxidative stress and inflammation

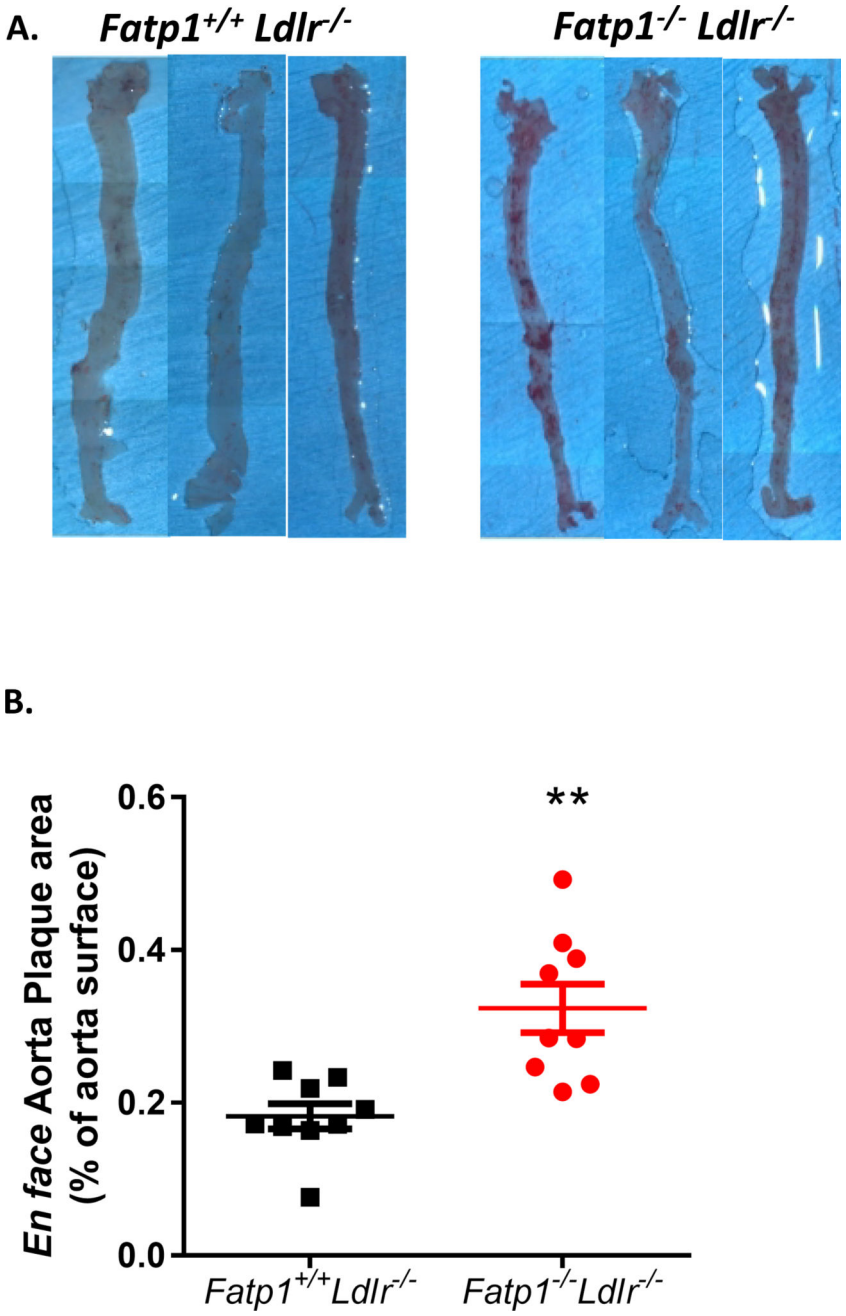

Fig. 1. *Fatp1*$^{-/-}$*Ldlr*$^{-/-}$ mice displayed increased atherosclerotic lesion size compared to *Fatp1*$^{+/+}$*Ldlr*$^{-/-}$ mice as determined by *en face* analysis

(A) *Fatp1*$^{+/+}$ *Ldlr*$^{-/-}$ or *Fatp1*$^{-/-}$*Ldlr*$^{-/-}$ aortas were isolated and stained with Oil red O. Representative images are shown. (B) Atherosclerotic lesion size was quantified using Image J software. Data are presented as means ± SEM, n =9. ***p*=0.001.

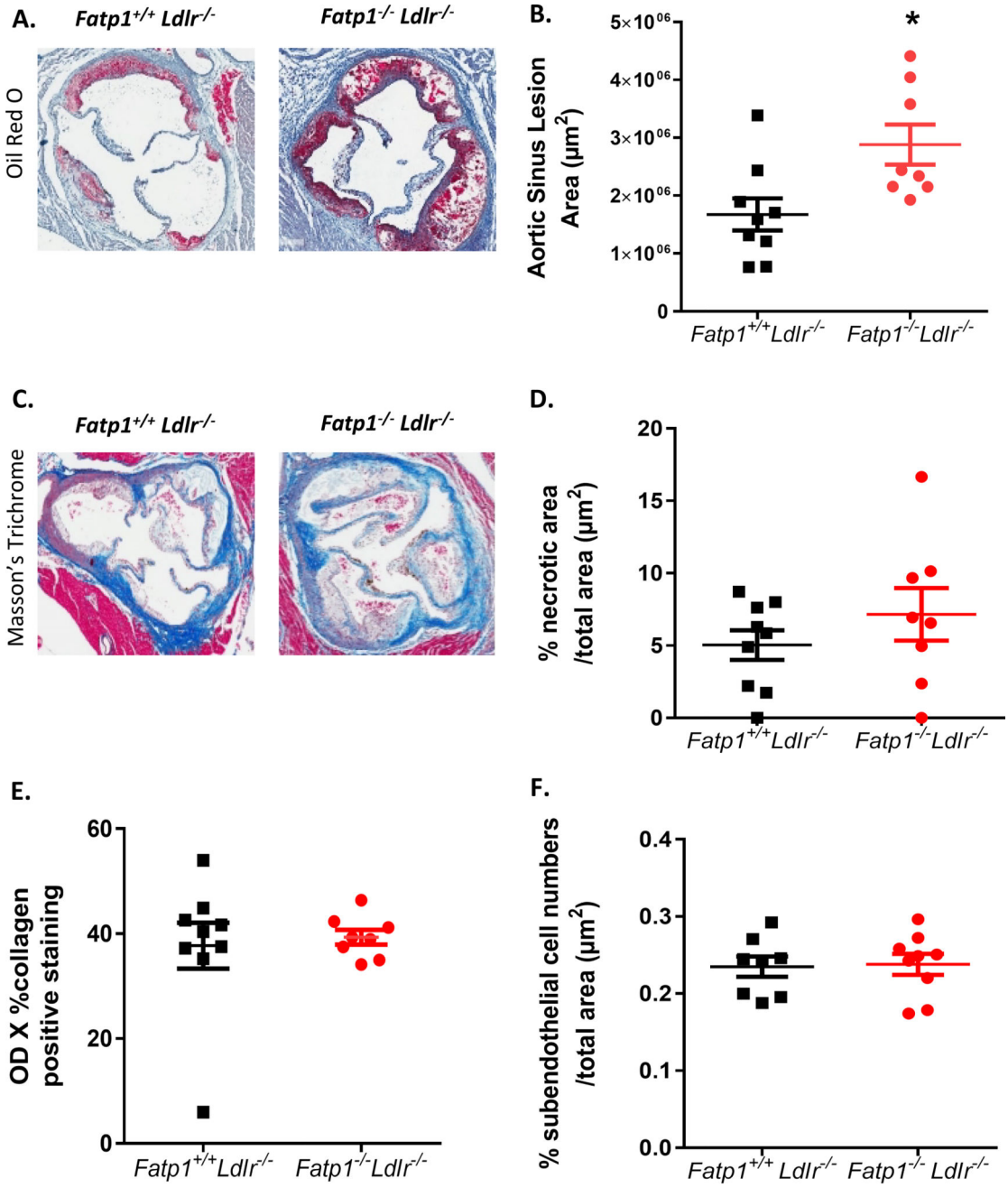

Fig. 2. Deletion of *Fatp1* increased atherosclerotic lesions in the aorta sinus but not necrosis or collagen deposition

(A) 20× representative photomicrographs of Oil Red O staining for $Fatp1^{+/+}Ldlr^{-/-}$ or $Fatp1^{-/-}Ldlr^{-/-}$ aortic sinus. (B) Atherosclerotic lesion size was quantified using Aperio ImageScope Software. (C) 20× representative photomicrographs of Masson's trichrome staining for $Fatp1^{+/+}$ $Ldlr^{-/-}$ or $Fatp1^{-/-}Ldlr^{-/-}$ aortic sinus. (D) %Necrotic area/total area in lesions was quantified using Aperio. (E) Collagen was quantified. (F) % Subendothelial cell numbers/total area in subendothelial space were quantified. Data are presented as means ± SEM, n = 8 or 9. *p=0.015

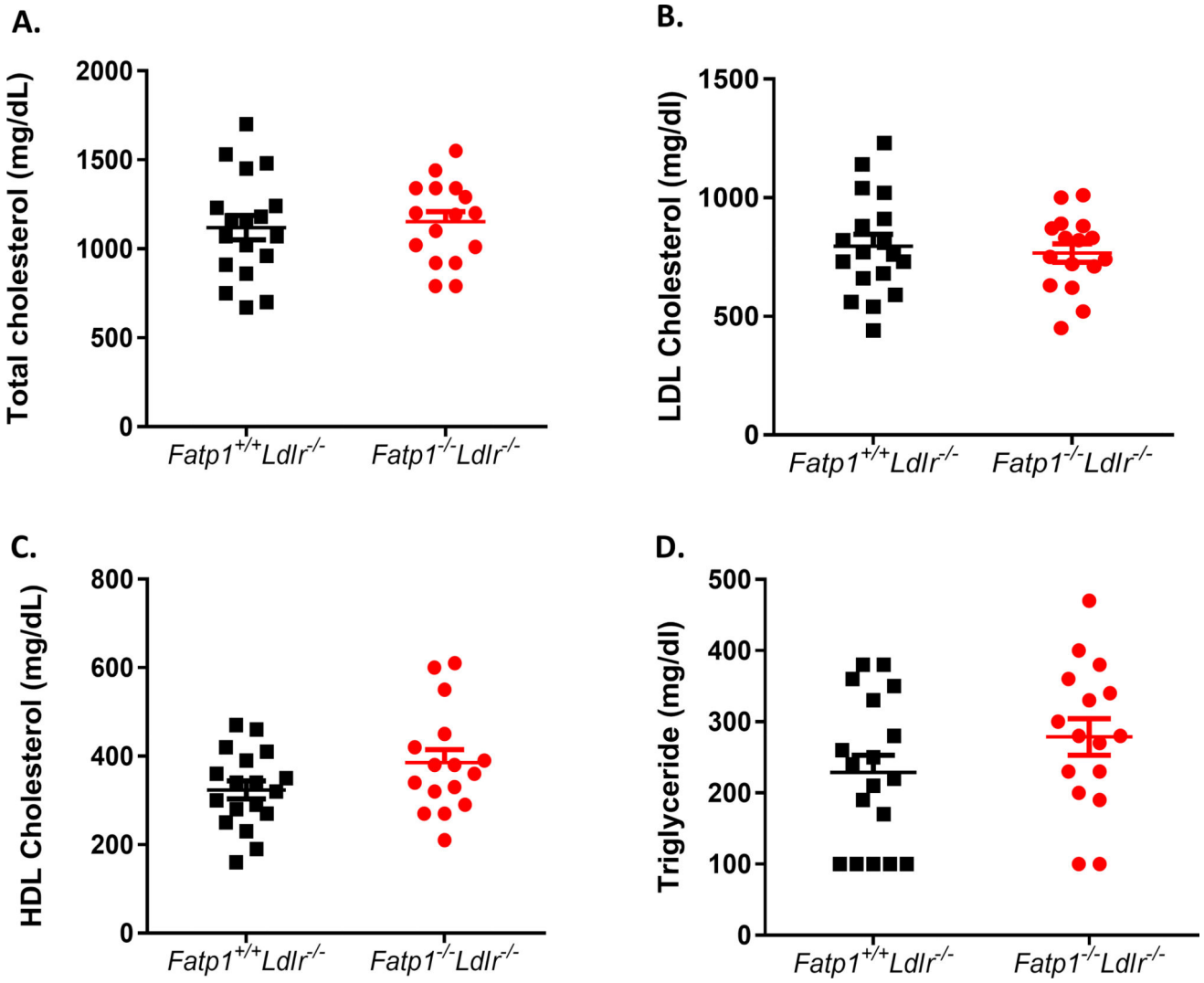

Fig. 3. *Fatp1*$^{-/-}$*Ldlr*$^{-/-}$ mice did not display alterations in plasma total cholesterol, LDL cholesterol, HDL cholesterol, and triacylglycerol concentrations compared to *Fatp1*$^{+/+}$*Ldlr*$^{-/-}$ mice

(A) Total cholesterol. (B) LDL cholesterol. (C) HDL cholesterol and (D) triacylglyceride. Data are presented as means ± SEM, n = 18 or 16.

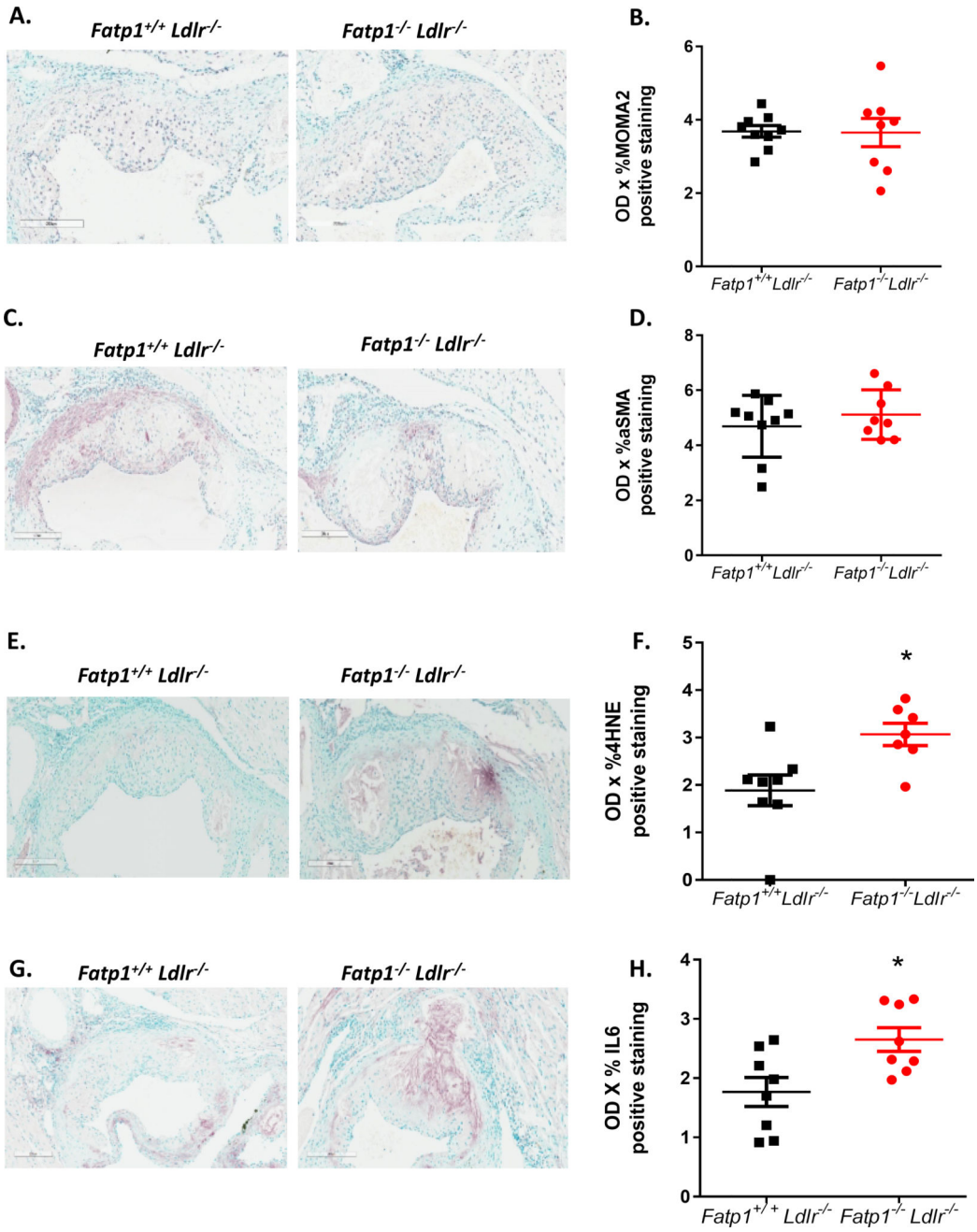

Fig. 4. Deletion of *Fatp1* increased atherosclerotic plaque oxidative stress without changing plaque cell composition

(A) 200 μm representative images of immunostaining macrophage marker MOMA2. (B) Quantification using OD × % MOMA2 positive staining. (C) 200 μm representative images of immunostaining SMC marker α-SMA. (D) Quantification using OD × %α-SMA positive staining. (E) 200 μm representative images of immunostaining oxidative stress marker 4HNE. (F) Quantification using OD × %4HNE positive staining. **p*=0.013. (G) 200 μm representative images of immunostaining inflammation marker IL6. (H) Quantification

using OD × %IL6 positive staining. *p=0.014. Data are presented as means ± SEM, n = 7 or 9.